



## Article

# An Approach to Obtaining Stable Parameter Estimates Using Experimentally Obtained Delay Values in a Cellular Mobile Network

Aleksandrs Kutins and Deniss Brodnevs\*

Institute of Aeronautics (AERTI), Riga Technical University (RTU), Riga, Latvia  
E-mail: [deniss.brodnevs@rtu.lv](mailto:deniss.brodnevs@rtu.lv)

Received: 13 April 2023; Revised: 3 May 2023; Accepted: 10 May 2023

**Abstract:** The ability to describe experimentally obtained delay values in a cell of a mobile cellular network allows not only describing the properties of cell delays using only a few parameters, but also to simulate delay values. Unfortunately, occasionally occurring temporary unstable operation of a cellular network, caused by various negative factors, leads to a noticeable increase in delays and, as a result, to a significant distortion of the obtained delay parameters estimates. For this reason, estimates of the delay parameters in a cell should be obtained from experimental data obtained at the time of stable operation of the network. Due to the large amount of experimentally obtained data, the process of checking experimentally obtained delay values for the presence of anomalies should be performed on the application of simple criteria. The aim of this paper is to show an approach to obtaining stable parameter estimates of delay in a cell of a mobile cellular network. The article describes the factors that affect delays stability, assesses the degree of their influence, and also highlights properties that can be used to recognize phenomena that adversely affect the value and stability of delays in order to exclude such experimentally obtained data from the evaluation.

**Keywords:** mobile cellular network, LTE, 4G, delays, performance evaluation, experimental evaluation, simulation, parameter estimates

## 1. Introduction

In the further development of mobile data transmission technologies of mobile cellular networks, the main attention was paid to increasing the data rates. Consequently, much less attention was paid to both the reliability of data transmission (the number of lost packets) and the data transmission delays (average delay, as well as packet jitter). With the development of remotely controlled robots (including mobile remotely piloted drones), the issue of using the data transmission service of cellular networks as a cheap and small-sized solution for the remote control and telemetry in vehicular networks has become relevant [1–4]. However, for the remote-control applications, the main parameters of the data transmission channel are reliability and delays of the commands [5–9]. Developers of the remote-control solutions need to have a tool which can be used to make sure that the selected cellular mobile operator network is able to provide communication with delays that do not exceed the limit defined by the manufacturers of the remotely controlled equipment, such as [10,11].

Very preliminary, delays in the data transmission service of the cellular mobile network can be estimated using the “ping” utility on the mobile terminal, where the terminal can be travelled around some territory (for example, by car outside of populated areas or, conversely, within a densely populated area – which is better for the manufacturer). There are many publications available containing reports of delays obtained by the above experimental method, for example [12–15].

The main disadvantage of such experimental approach is that the aforementioned research results are generalized, i.e. mean values are found or a Cumulative Distribution Function (CDF) of delays in the cellular network is constructed. Such approach is not entirely correct, since in modern cellular networks a User Equipment (UE) can operate with only one Base Station (BS) at a time, and not with all network at once: a UE will transmit the data with the delays of a particular cell, and not with the average delays of the entire cellular mobile network (see Figure 1 for more details). At the same time, the cell performance largely depends on the implementation of the terrestrial backhaul link (which also is called a “first mile link”) connecting BS with the core network, and the implementations of the terrestrial backhaul interface can be various: from fibre optic cables (usually used in densely populated areas) to multi-hop radio links (usually used in rural areas) [16]. Further, the modulation and coding scheme of a UE is dynamically selected according to the quality of a radio signal. Therefore, the quality of the radio signal also affects the delays of data transmission.

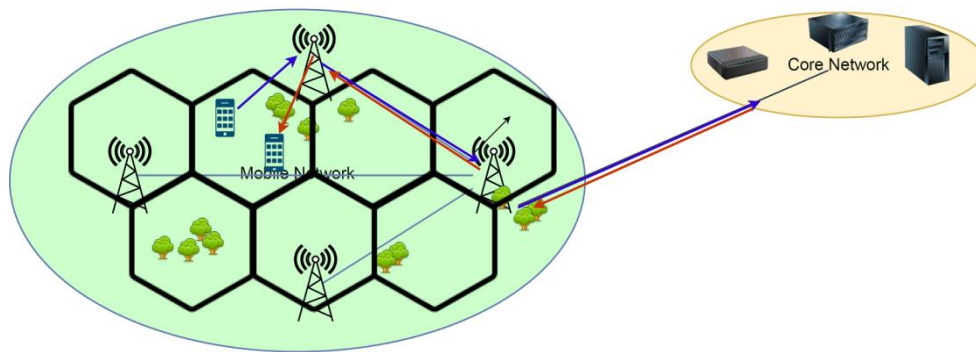


**Figure 1.** All traffic goes through the Core Network (CN) even if the source and the destination UEs are within the same cell.

Therefore, the delays in a cellular network should be estimated in each cell separately, like it has been done (but not highlighted) in [17–20]. The quality of the radio signal must also be taken into account because it affects the choice of the modulation and coding scheme of a radio segment. Note that since the selection of the modulation and coding scheme is based on measurements of the radio signal quality made by the UE itself [21,22], it is advisable to use the radio signal quality indicators reported by the UE itself.

In order to be able to conveniently evaluate the delay values experimentally obtained within a cell, as well as to be able to simulate the delay values, a tool is needed that allows one to describe the delay values with satisfactory high accuracy and acceptably low complexity.

Delays in a cell can be described by a mixture of distribution functions: for example, delays in an LTE cell can be described by a mixture of four unimodal distribution functions [18]. This approach allows to achieve a high quality of delay values fit. However, the process of obtaining parameter estimates and distribution weight coefficients must be performed for each set of delays from each cell separately, which make the process time and resource consuming.

If the goal is to describe only some of the properties of delays in a cell, then the most appropriate unimodal distribution law can be found. In particular, average delay and delay jitter in an LTE cell can be described with sufficient accuracy, assuming that the delays in an LTE cell obey the log-normal distribution law [23]. In this case, the parameters of the log-normal distribution law should be determined from the delay values obtained with “sufficient” signal quality (that is, when the SINR value does not have a noticeable effect on the delay values), and the network must operate without failures and congestions.

In order to improve the accuracy and repeatability of obtained parameter estimates of the log-normal distribution, the values that significantly differ from other population, should be discarded from the entire set of experimentally obtained values of cell delays. To do this, it is proposed to impose an upper limit of three standard deviations. It is stated [23] that if the quality of the radio signal is “sufficient” (SINR values are within certain limits), and local delay values spikes (congestion) are discarded (i.e. temporary network failures and congestion, as well as short-term adverse effects of fading (small-scale fading) are discarded from the analysis), then the use of the log-normal distribution law makes it possible to obtain estimates of the average delay value with an error of 0.5%, and IPDV (jitter) values with an error of 20%.

This article is devoted to determining the degree of influence of the radio signal quality (SINR) on the delays in a cell. Next, we will look at various negative effects that cause a sharp increase in delays (even if the SINR is “good”), and consider signs and properties that can be used to determine whether this negative effect occurred at the time the delay values were obtained. These signs and properties can be used to exclude the experimentally obtained delay values from the analysis if they contain locally increased delays due to congestion or cell overload.

## 2. Experimental Estimation of the UE to UE Delay Dependence on Signal Quality

Since various BSs can have different terrestrial backhaul, the experimental evaluation should be carried out within a single cell. For this, UEs must be equipped with the same cellular operator sim cards, locked on the same frequency band and registered within the same cell. The source and destination UEs antennas must be equally aligned to each other and spaced by not so great distance (say, 1 meter from each other) to have almost the same signal quality. Both UEs must report radio link performance KPIs as well as cell in use.

The variations for the signal quality can be obtained by transporting UEs, say, by a car. To cancel the impact of different terrestrial backhaul links implementations of BSs, the experimental data for a particular packet size must be captured within the same cell. ICMP packets may be used to eliminate the effect of retransmissions by the TCP and Radio Link Control – Acknowledged Mode (RLC AM) retransmission mechanisms. Note that even when using ICMP packets, the air interface remains protected by the Hybrid Automatic Repeat Request (HARQ) fast retransmission mechanism (see Figure 2 for more details).

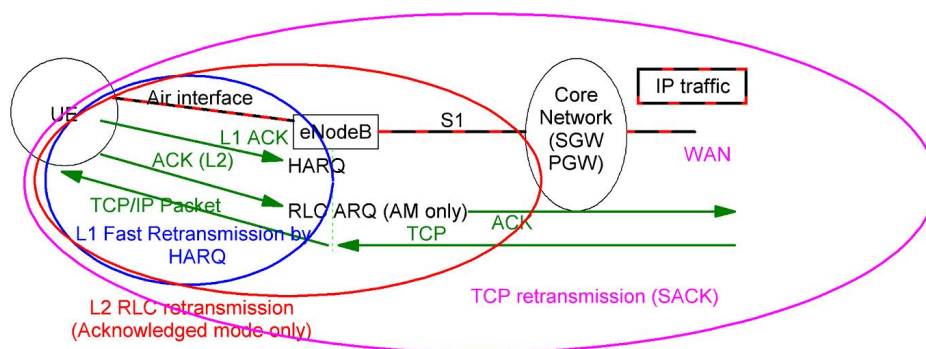


**Figure 2.** The HARQ mechanism protects all traffic through the air interface, whereas TCP and RLC-AM retransmissions are for the protected traffic only.

### 2.1 Average Delay Dependence on Signal Quality

As an example, the LTE Cat. 4 USB dongles Huawei 3372h were used. The ICMP packets were used to eliminate the impact from TCP and RLC-AM retransmission mechanisms. Two packet payload values were chosen: 100 bytes and 1472 bytes respectively. The echo request was sent at a rate of 10 Hz, but each subsequent request was sent only if the previous request had got a reply. That is, if the Round-Trip Time (RTT) was greater than 100 ms, then the send rate was below 10 Hz. The uplink and downlink data rates were up to 10 kbps and 120 kbps for 100 and 1472 bit payloads respectively. Radio channel performance KPIs and active cell ID (CID) were reported by both LTE dongles. The radio channel KPIs, CIDs and delay RTT values were captured, decoded and stored by the custom-made application. The application is implemented in NI LabView environment. Refer to Figure 3 for more details.

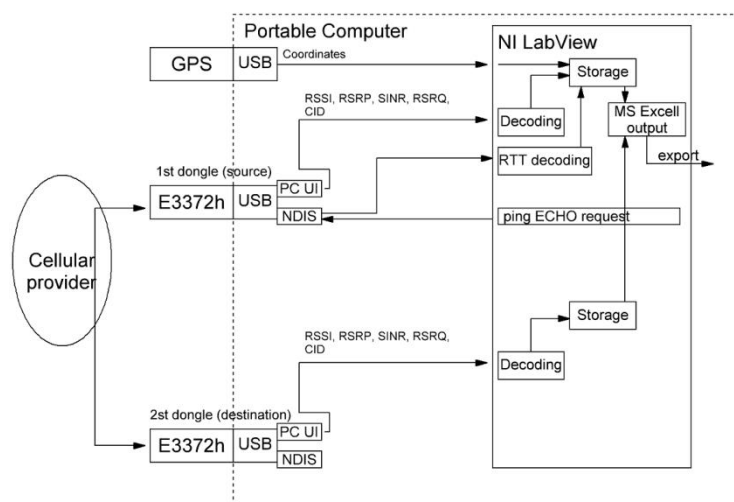


**Figure 3.** Experimental setup used in all experiments.

The dependence of the RTT delay average value on SINR was experimentally obtained by performing measurements between two LTE dongles located in a car. The LTE dongles were equipped with SIM cards from the same mobile cellular operator and were locked to the B20 band (800 MHz). Two mobile cellular operators were used in the experiment, thus two sets of experimentally obtained data were received, processed and further synchronized and combined to obtain the results. RTT values were grouped by SINR value, and further, an average value was taken from each set. The delay sets were analyzed separately for each cell in order to eliminate the influence of different implementation of BS terrestrial backhaul links on the average delay. The values when the UEs were not registered within the same cell were ignored. Because both UEs were located within 1 meter of each other in the car, the reported SINR may differ slightly. In our case, each SINR value for the processing is calculated as a minimum value from a pair of SINR values reported by both UEs. Since different cells may have different average delays, the deviation from the relative average delay was calculated to obtain comparable results.

Figure 4 shows the average relative deviation of the average RTT in cells for packets with a payload of 100 bytes (packet size 128 bytes) per particular SINR from the average RTT. Since the dongles send reports with signal parameters with some delay, two sets of data were captured: the first was obtained when travelling speed was in the range of 40 ÷ 100 km/h and, thus, the delay in SINR reporting can be comparable with the rate of change in propagation conditions; the second – at a speed of 7 km/h. For clarity, both datasets are shown on the same plot; the outage threshold below which the UE may lose service is shown at SINR = -6 dB [24].

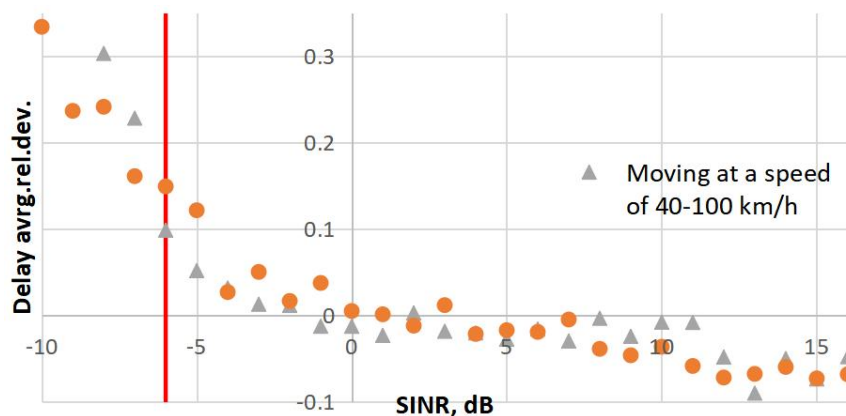


Figure 4. Relative deviation of an average RTT vs SINR for 128 Bytes packets.

As can be seen, the difference between the two sets of data obtained at different driving speeds only appears at very low SINR values: UEs were able to operate at SINRs down to -10 dB if the driving speed was only 7 km/h, while at higher driving speeds — only down to -8 dB SINR. Above the outage threshold of -6 dB SINR, there are no significant differences between the two data sets, so it can be concluded that the experimental data can be obtained at driving speeds up to 100 km/h. Consequently, all further experiments will be carried out without taking into account the driving speed.

Figure 5 shows the average relative deviation of the average RTT in cells for packets with a payload of 1472 bytes (packet size 1500 bytes, thus equal to MTU) by a particular SINR from the average RTT. The driving speed was in the range from 10 to 100 km/h, depending on road conditions.

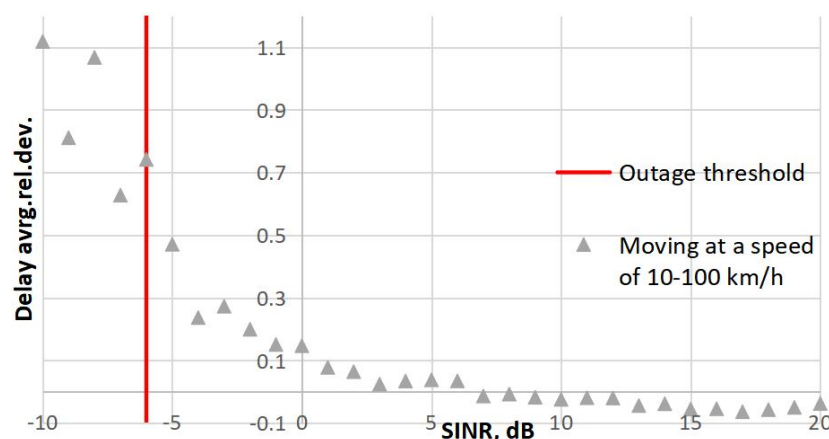


Figure 5. Relative deviation of average RTT vs SINR for 1500 Bytes packets.

As can be seen, the RTT values for 128-byte packets do not depend on the signal quality (the difference is within 5%) if the SINR is in the range from 0 to +10 dB, and also from +12 to +24 dB. RTT values for 1500 B packets (1472 payload bytes) are independent on the signal quality (within 5% difference) if the SINR is between +3 to +6 dB, +7 to +12 dB, and +13 to +20 dB.

Using multiple sets of SINR ranges can greatly complicate all further analyses. Thus, the area of interest was found by collecting statistics on the SINR values reported by the dongles during travelling. Figure 6 shows the PDF and CDF of SINR values taken from a continuously moving car in both populated and rural areas.

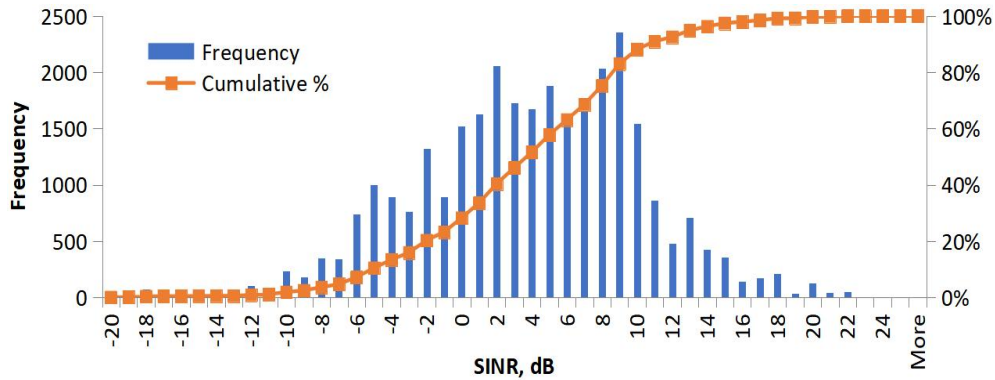


Figure 6. PDF and CDF of the SINR values.

Since very high SINRs (i.e. 10 dB and above) are much less common than average SINRs (i.e. -3 to 10dB), and in order to consider less favorable conditions in terms of network delays, it was decided to ignore the RTT values obtained at the "high" SINR; Of course, since low signal quality negatively affects delays and their stability, RTT values obtained at "low" SINR will also not be used. Table 1 shows the boundary conditions for the SINR values under which it can be assumed that the delay values do not depend on the quality of the radio signal. Further, the signal quality will be referred to as "good" if the SINR values are within these limits set for the respective packet sizes.

Table 1. SINR range, which does not affect delay values

Packet size, Bytes	Minimum SINR, dB	Maximum SINR, dB
128	0	+10
1500	+4	+12

## 2.2 Maximum Delay Dependence on Signal Quality

The signal quality expressed in SINR affects not only the coding and modulation scheme of a UE (and thus the data rate over the air interface), but sometimes also the number of packets retransmitted by the HARQ mechanism (due to increased packet loss if the signal is noise or interference limited) [21].

Figure 7 and Figure 8 show the average relative deviation of the maximum RTT in cells for 128 Bytes and 1500 Bytes packets respectively, per specific SINR from the maximum average RTT. The maximum RTT values were obtained as 99% percentiles of delay values for each cell. The driving speed was in the range from 10 to 100 km/h.

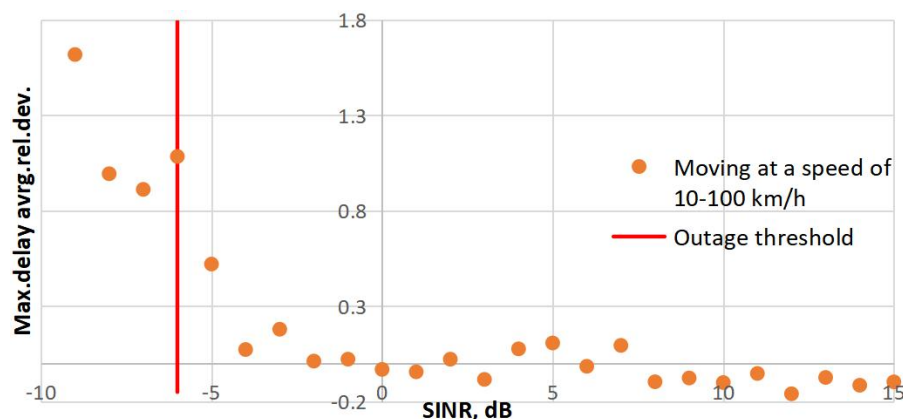


Figure 7. Relative deviation of maximum RTT vs SINR for 128 Bytes packets.

As can be seen, even if the data transfer service remains operational down to  $-6$  dB SINR (sometimes even lower), the maximum delay values become noticeably increased if the SINR value is below 0 dB.

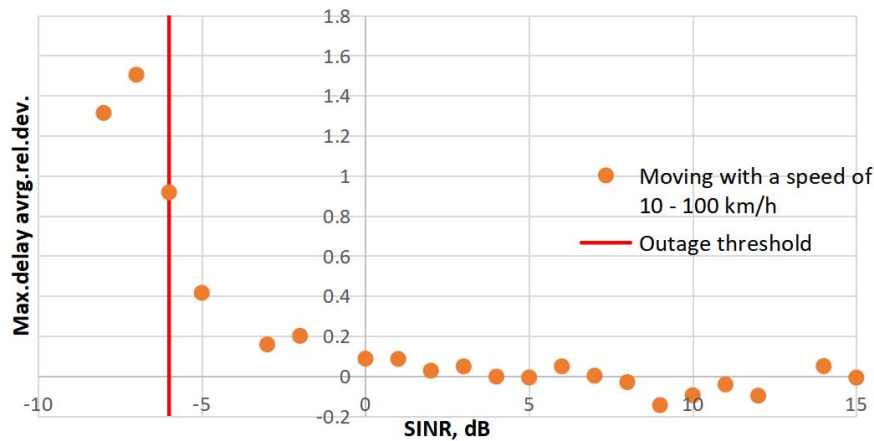


Figure 8. Relative deviation of maximum RTT vs SINR for 1500 Bytes packets.

### 2.3 Approximation of the Average and Maximum Delay Dependences on Signal Quality

As stated above, delays in an LTE cell can be described with a log-normal distribution if the radio signal quality is "good". The term "good signal quality" means that the SINR is in the range shown in Table 1. If the SINR falls below the minimum threshold shown in Table 1, the delays will increase. The degree of increase in the average delay can be approximated using a polynomial approximation. Figure 9 and Figure 10 show the dependence of the relative deviation of the average cell delay on SINR for various packet sizes. An approximation using a polynomial function is also shown.

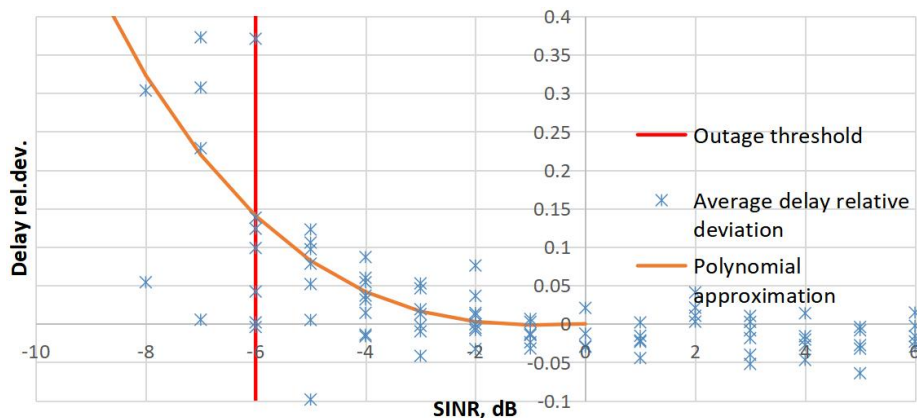


Figure 9. Relative deviation of average delays in various cells for 128 Bytes packets.

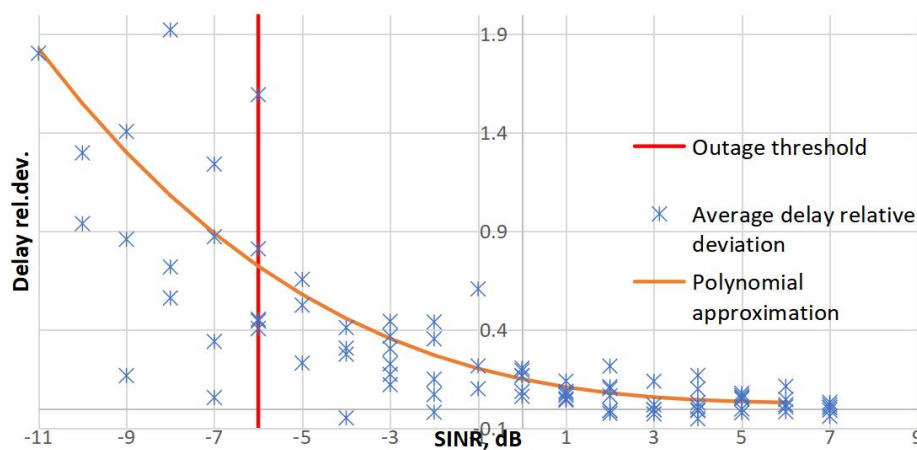


Figure 10. Relative deviation of average delays in various cells for 1500 Bytes packets.

As shown in Figure 7 and Figure 8, the maximum delays in an LTE cell also increase significantly due to multiple retransmissions if the SINR falls below a certain minimum threshold given in Table 1. The increase rate can also be approximated with a polynomial function. Figure 11 and Figure 12 show the relative deviation of the 99 % percentile of delay in each cell versus SINR for various packet sizes. An approximation using a polynomial function is also shown.

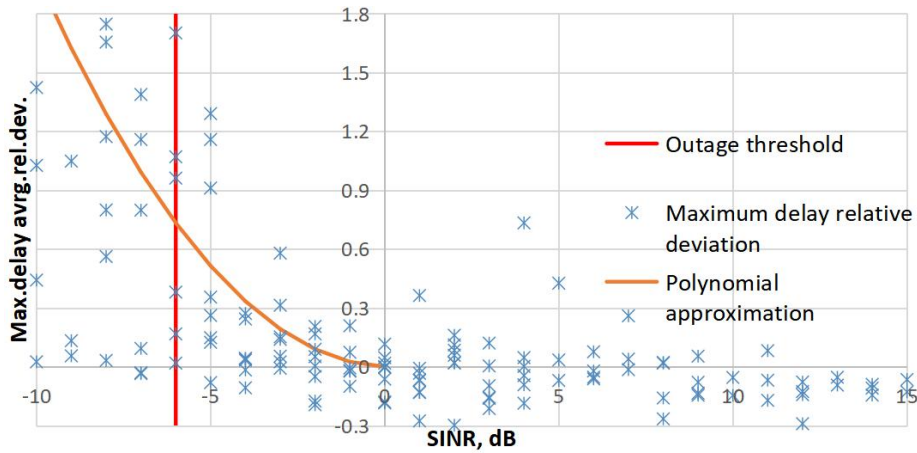


Figure 11. Relative deviation of maximum delay for 128 Bytes packets.

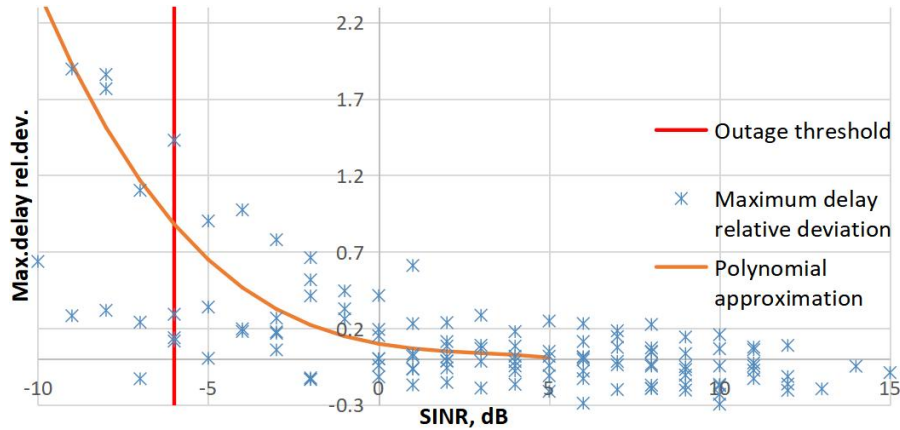


Figure 12. Relative deviation of maximum delay for 1500 Bytes packets.

In all cases the third-degree polynomial approximation was used.

$$\frac{\overline{\text{delay}}_{\text{SINR}} - \overline{\text{delay}}_{\text{goodSINR}}}{\overline{\text{delay}}_{\text{goodSINR}}} = a_3 \cdot \text{SINR} + a_2 \cdot \text{SINR} + a_1 \cdot \text{SINR} + a_0 \quad (1)$$

where SINR is a particular SINR value,  $\overline{\text{delay}}_{\text{SINR}}$  is an average delay value at a particular SINR value,  $\overline{\text{delay}}_{\text{goodSINR}}$  is an average delay value calculated from delay values obtained when the SINR was as specified in Table 1.

The polynomial coefficients and applicability limits are given in Table 2.

Table 2. Coefficients of the polynomial approximations for low SINR negative effect estimation on average and maximum delays.

Parameter	Applicability	$a_3$	$a_2$	$a_1$	$a_0$
Average delay, 128 Bytes packet	SINR $\leq$ 0 dB	-0.005	0.0015	0.0036	0
Average delay, 1500 Bytes packet	SINR $\leq$ 4 dB	-0.0003	0.0063	-0.0468	0.15
0.99 percentile delay, 128 Bytes packet	SINR $\leq$ 0 dB	0	0.0194	-0.0058	0
0.99 percentile delay, 1500 Bytes packet	SINR $\leq$ 4 dB	-0.001	0.0092	-0.0389	0.1

### 3. Experimental Estimation of the UE to UE Delay Parameters

The previous chapter showed that the delay values are independent on the quality of the radio signal, if the SINR value is within the limits given in Table 1. Another source of concern is the stability of delay properties (and thus parameters too) in a particular cell under constant signal propagation conditions (for example, when UE is immovable). Since the topology of the terrestrial backhaul of the cellular network operator is unknown, all dependencies can be found only experimentally. Existing methods allow to identify possible anomalies in the mobile data transfer service with high percentage of probability [25–28]. These approaches are based on the use of specific transport or signaling layer information (which typically is not accessible through typical UE) or on the machine learning algorithms.

We suppose that the processing of a large experimentally obtained data set should be processed with less complex algorithms. Therefore, we will attempt to find less complex properties of delays sets (i.e. mean, standard deviation and skewness estimates) that can be used to identify possible anomalies such as abnormally increased delay values due to temporary congestion or failure in a network. For this, several sets of delay values were obtained experimentally. RTT was measured between two dongles that were registered in the same cell. Two LTE cat. 4 Huawei 3372h USB dongles were placed in buildings for a certain period of time. Both were equipped with SIM cards from the same cellular network operator and were configured to use the same technology (LTE) and the same frequency band (B3 or B20). The distance between them in each experiment was one meter. As in previous experiments, the dongles reported cellular network parameters such as SINR, RSRQ, and the CID of the cell in use.

Differences in the values of point estimates of the distribution parameters of delay values obtained in the same LTE cell, but at different time of the day, are due to several factors. First, if delay measurements are made from a moving vehicle outside of populated areas, then the typical time spent in one cell will be on the order of 2 minutes; therefore, assuming that the average delay is 100 ms, and measurements are made at the highest possible frequency, then the number of delay values obtained in one cell will be about one thousand. After excluding the delay values obtained with SINR values that do not meet the requirements specified in Table 1, taking into account the statistics from Figure 6, approximately six hundred delay values remain. And if the route runs close to the border between cells, then the number of received delay values can be even less, which leads to an increase in random errors in determining parameter estimates. The second reason may be a highly variable load on the cell, as well as temporary failures or congestions in the operation of the BS terrestrial backhaul as it is shown in Figure 13. In the next chapters we will take a closer look to each behaviour separately.

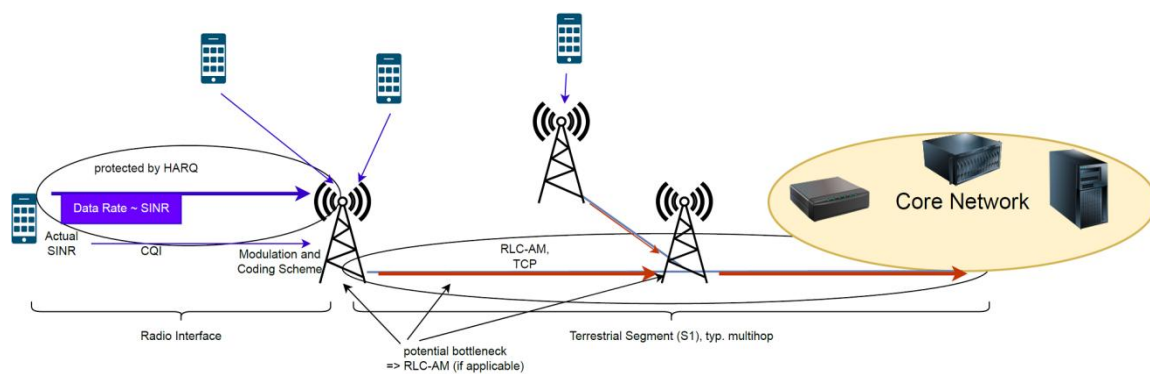


Figure 13. Potential bottlenecks are in the terrestrial backhaul.

#### 3.1 Estimates of Delay Parameters in a Cell

Assuming that there are no local overloads (i.e., local bursts of sharply increased delay) and bursts of significantly increased standalone delay values (i.e., values that go beyond the confidence level of three standard deviations), and also under the condition that the signal quality is “good” (i.e. SINR is within the range specified in Table 1), delays in an LTE cell can be approximated by a log-normal distribution [23]. Accepting the hypothesis that the delays in a cell  $cell_a$  obey the log-normal distribution, further we will use the following definitions of parameter estimates (expected values  $\hat{\mu}_{cell_a}$ , standard deviation values  $\hat{\sigma}_{cell_a}$ , skewness  $\hat{S}k_{cell_a}$ ), where  $n$  is number of delay values within a cell  $cell_a$ , obtained when SINR was “good”:

$$\hat{m}_{cell\_a} = \frac{\sum_{i=1}^n \ln(\text{delay}_{cell\_a_i})}{n} \quad (2)$$

$$\hat{\sigma}_{cell\_a} = \sqrt{\frac{\sum_{i=1}^n (\ln(\text{delay}_{cell\_a_i}) - \hat{m}_{cell\_a})^2}{n-1}} \quad (3)$$

$$\hat{Sk}_{cell\_a} = \frac{n}{(n-1)(n-2)} \sum \left( \frac{\ln(\text{delay}_{cell\_a_i}) - \hat{m}_{cell\_a}}{\hat{\sigma}_{cell\_a}} \right) \quad (4)$$

### 3.2 Estimates of Delay Parameters in a Cell with a Stable Load

Even if the delays in a cell are stable, with a small number of measured values  $n$ , the obtained point estimates of the delay parameters are largely random and may differ greatly from the true value of the distribution parameters of the delay values in a given cell due to insufficient number of experimentally obtained data. Let's illustrate this situation with the following example: there are experimentally obtained delay values from one LTE cell for the UE to UE connection. Both UEs were stationary located in a building in an industrial district. Both UEs were registered in the same cell. Delays were measured once per second for 15 hours; ICMP packet size was 124 Bytes; the SINR values of both UEs were within the limits recommended in Table 1 for 128 Bytes packets, and the RSRQ values were within  $-6 \div -10$  dB. For clarity, Figure 14 also shows the average delay value obtained as moving average from 50 values.

Looking at the average delay values obtained by averaging fifty adjacent delay values, one might get the impression that the average delay per cell has fluctuations. However, this may not be the case, since fluctuations in the values of the average delay can only be due to random factors caused by a small number of measurements ( $n$  is only fifty). This hypothesis can be tested by superimposing a confidence interval on the values of the mean delay estimate. But we, for clarity, will use a slightly different way of illustration. So, let's assume that delays in an LTE cell obey a log-normal distribution. Let us obtain estimates of the distribution parameters for the entire set of experimentally obtained delay values and assume that they are equal to the distribution parameters:  $\hat{\mu} = \mu = 4.236300673$ ,  $\hat{\sigma} = \sigma = 0.203821802$ . Now we obtain the values of point estimates of the distribution parameters using  $n = 50$  neighboring delay values. The values of the parameters point estimates  $\hat{\mu}_{50}$  and  $\hat{\sigma}_{50}$  will be plotted on a two-dimensional graph and shown in Figure 15. We then generate three hundred thousand delay values using the parameter estimates  $\mu = 4.236300673$  and  $\sigma = 0.203821802$ . Since the random variable is infinite by definition, we will impose a confidence ellipse on the obtained values with a confidence probability  $\beta = 0.997$ .

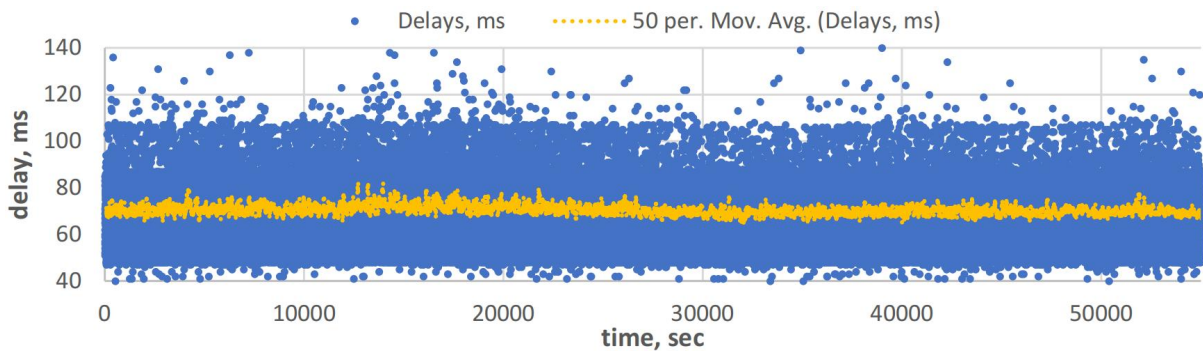


Figure 14. Delay values and running average ( $n = 50$ ) in the LTE cell with stable delay.

As can be seen, despite the fact that the values of the distribution parameters were unchanged, the parameter estimates obtained from the  $n = 50$  generated values have some scatter (see “simulated” markers on Figure 15).

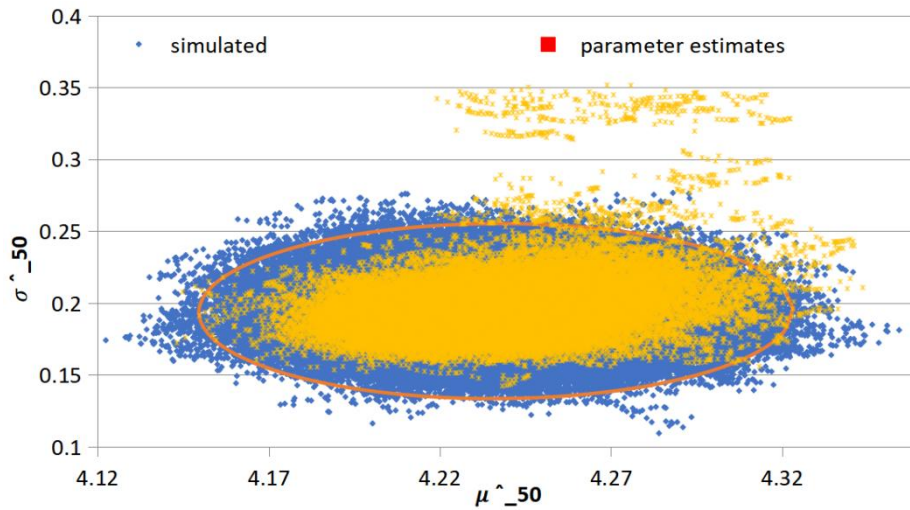


Figure 15. Parameter estimates from the experimental and simulated data.

According to the central limit theorem, for a large number  $n$ , the distribution law of the sum of identically distributed random variables is close to normal. Then, assuming that the values of the estimates are distributed according to the normal law, we will impose a confidence ellipse (in our case, built for the confidence probability  $\beta = 3\tau = 0.997$ ) on the values of the parameter estimates obtained from generated values using  $n = 50$  neighbor values. It can be seen that 99.67% of the  $\hat{\mu}_{50}$  estimates, obtained from the experimental data, fall into the same ellipse, where the parameter estimates also were estimated using  $n = 50$  neighbor values. The same cannot be asserted about the  $\hat{\sigma}_{50}$  estimates, because 1.51% values are outside the confidence interval.

Therefore, we can conclude that the fluctuations in the estimates of the parameter  $\hat{\mu}_{50}$  are caused by an insufficient number of measurements (in this example,  $n = 50$ ), while the fluctuations in the values of the  $\hat{\sigma}_{50}$  estimates in addition are caused by side factors.

### 3.3 Estimates of Delay Parameters in a Cell with Temporary Congestions

Link failures, temporary short-term overloads, as well as switching between flows in the operation of terrestrial backhaul lines of BSs, as a rule, do not lead to massive packet losses. This is achieved by the operation of lost packet resending mechanisms of terrestrial backhaul segment. However, as a result of the operation of such mechanisms, there will be packets with increased delays. One such experimentally obtained congestion is illustrated in Figure 16.

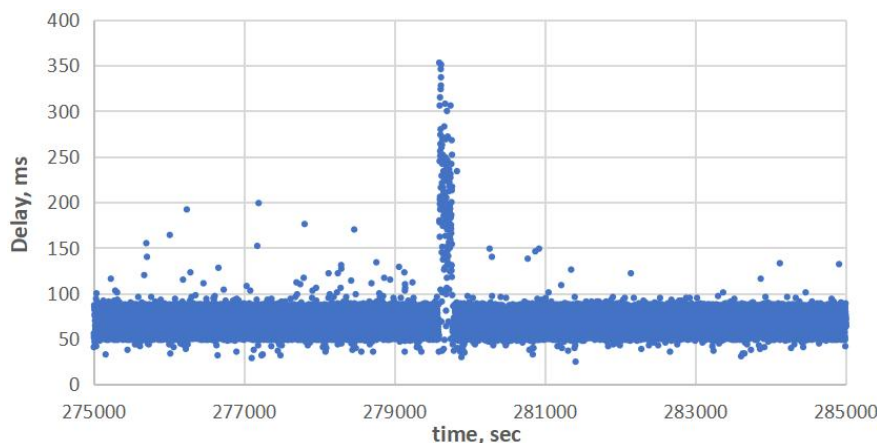


Figure 16. Illustration of the congestion effect on delays within a cell.

Let's consider delays at the moment of congestion in more detail (see Figure 17).

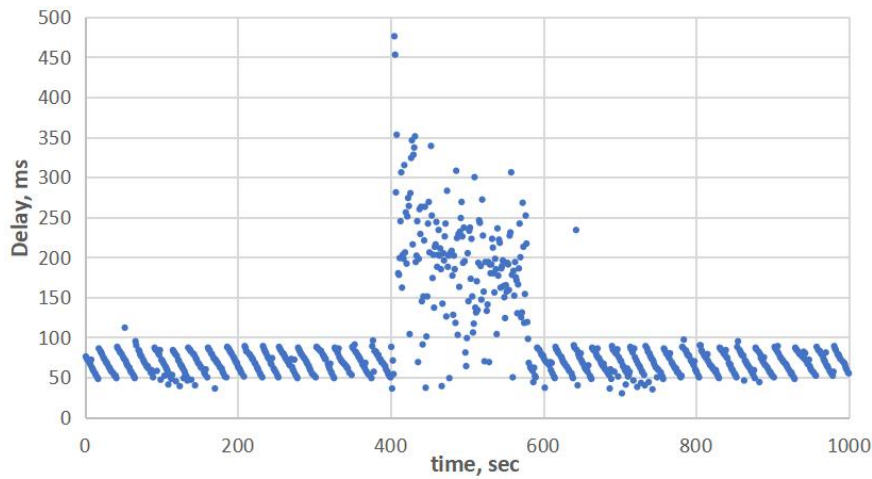


Figure 17. Delays during congestion in a BS backhaul.

As can be seen in figure 17, not all delay values are increased at the moment of congestion: some of them have values comparable to the delays before the congestion. This allows us to conclude that it is a congestion, and not a complete short-term failure of the connection. However, the same fact complicates the algorithm for detecting the congestion phenomenon. As an illustration, Figure 18 shows the cumulative distribution functions (CDFs) of the relative delay increase at the time of congestion versus the average delay before congestion occurs. The durations of each of the five congestions are also shown. All the congestions were obtained experimentally by measuring delays in cells during several week periods. The SINR readings at the time of obtaining the experimental data were consistent with the recommendations given in Table 1.

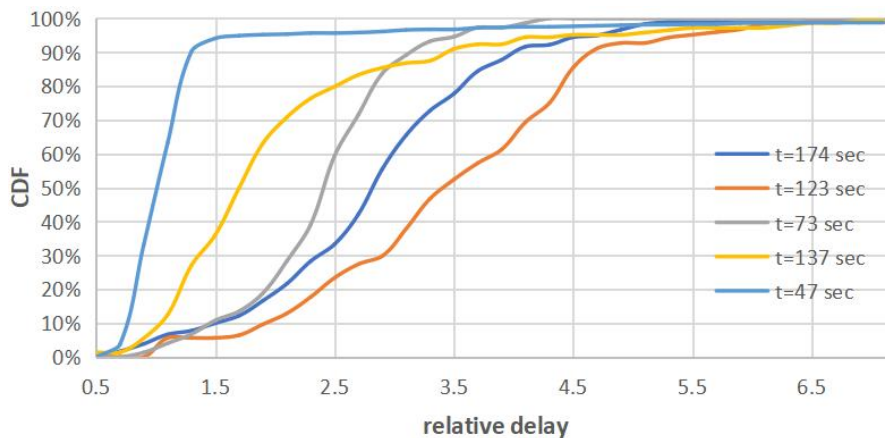


Figure 18. Relative increase of UE-to-UE delay during five experimentally captured congestions, ICMP packet size = 124 Bytes.

As can be seen from the presented five experimentally obtained cases, the duration of the congestion in some cases can exceed two minutes.

Let us illustrate the estimates (expected values  $\hat{\mu}_n$ , standard deviation values  $\hat{\sigma}_n$  and skewness  $\hat{S}k_n$ ) obtained using  $n$  neighbor delay values for a congestion lasting 123 sec. The delay values during congestion are shown in Figure 19 and running parameter estimates in Figure 20. Let us assume that delays in the absence of congestion and the presence of a “satisfactory” signal quality (refer to Table 1) obey a log-normal distribution. Note that the delay measurements were made once per second.

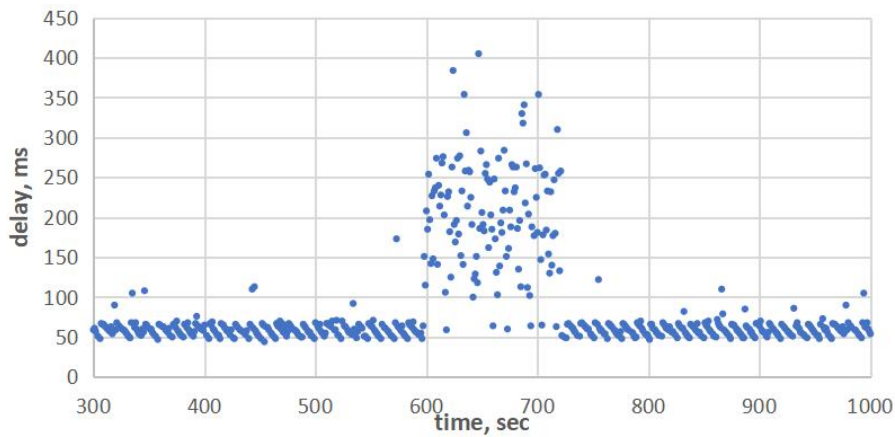


Figure 19. Delay values during 123 sec long congestion.

As can be seen, estimates of the of the expected values  $\hat{\mu}_n$  depend significantly on the number of measurements  $n$  that are used to determine the estimate, and the more measurements are used, the less the impact of increased delays caused by the congestion on the estimated value. Unlike  $\hat{\mu}_n$ , the standard deviation estimates  $\hat{\sigma}_n$  do not have such a strong dependence on the number of measurements  $n$ : the  $\hat{\sigma}_n$  estimate value remains increased both if the measurement period is less than or even longer than the congestion duration. Such an assumption can be accepted only if the duration of congestion is commensurate with the duration of observations, i.e. several hundred measurements  $n$  are captured during several minutes and the overload duration is up to 2 minutes. The skewness  $\hat{S}k_n$  estimated values normally are positive. The  $\hat{S}k_n$  remains positive even when estimated from a sample that includes congestion. However, it becomes negative if it is estimated exactly at the moment of congestion, if there are many significantly delayed packets in the congestion. Note that if the number of significantly delayed packets during congestion is not significant, the  $\hat{S}k_n$  value remains positive.

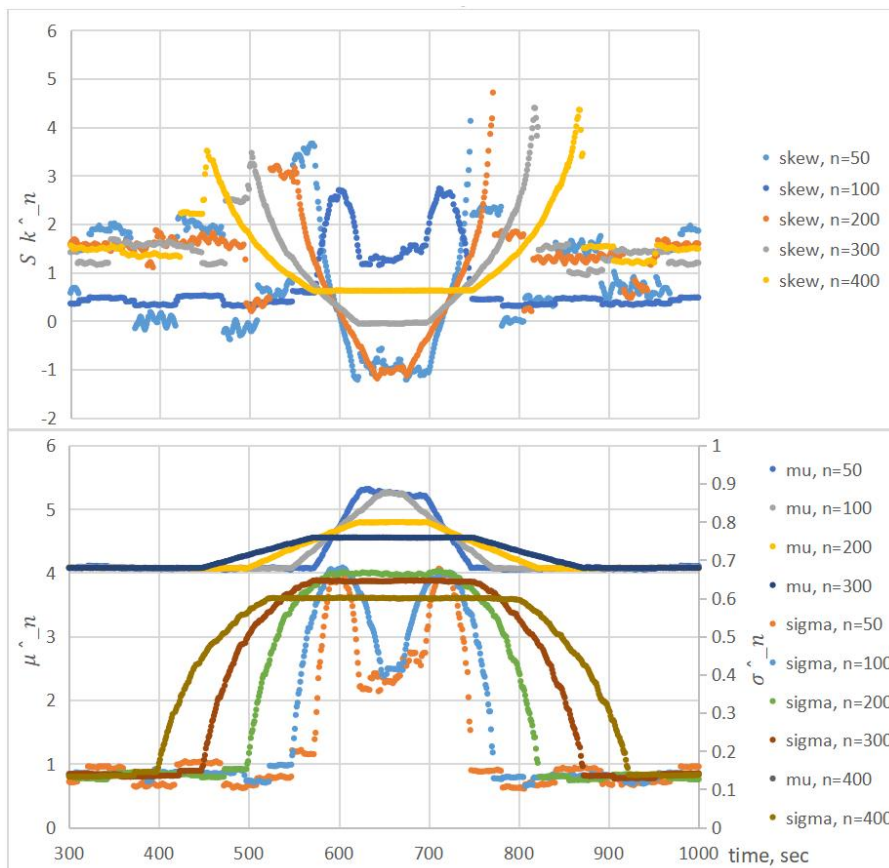


Figure 20. Parameters estimates during congestion for various sample size  $n$ .

Therefore, the degree of increase in the value of estimate  $\hat{\mu}_n$  obtained at the time of congestion significantly depends on the combination of the congestion duration and the overall duration of the measurement  $n$ , while estimate  $\hat{\sigma}_n$  obtained at the time of the congestion turns out to be increased almost independently of the combination of the duration of a congestion and the duration of measurements. However, the extent to which the estimate  $\hat{\sigma}_n$  increases depends on whether it is obtained from data that includes both normal operation and congestion, or only congestion. So, if estimate  $\hat{\sigma}_n$  is obtained from data that includes only congestion, its value does not increase so significantly. Let's make a reservation that speaking about the measurements duration  $n$ , it is considered that the measurements are made from a moving car, therefore the duration of measurements is only a few minutes, i.e. commensurate with the duration of the congestion. If the duration of measurements is incommensurably longer than the duration of congestion (for example, several hours compared to several hundred seconds of the congestion duration), then the conclusion about the increase in the value of the estimate  $\hat{\sigma}_n$  will be incorrect. In turn, the value of the skewness estimate  $\widehat{Sk}_n$  becomes negative if the estimate is obtained from delays at the moment of congestion.

### 3.4 Estimates of Delay Parameters in a Cell with Overloads

When the serving BS is heavily loaded, the cell delays also have the dependence on the BS load, even if the downlink SINR value is satisfactory. In this case, both temporary slightly increased values of delays as well as bursts of strongly increased delays will be observed.

Let us illustrate the operation of such a cell. Delay values were obtained experimentally by placing both UEs in a university campus. The ICMP packet size was 124 Bytes. Both UEs were registered in the same cell. Delays were measured once per second during four days period. The UE reported SINR values were within those recommended in Table 1, RSRQ was within  $-6 \div -11$  dB. Figure 21 shows RTT delay values measured between UEs, as well as the average delay found as running average of one hundred fifty adjacent values.

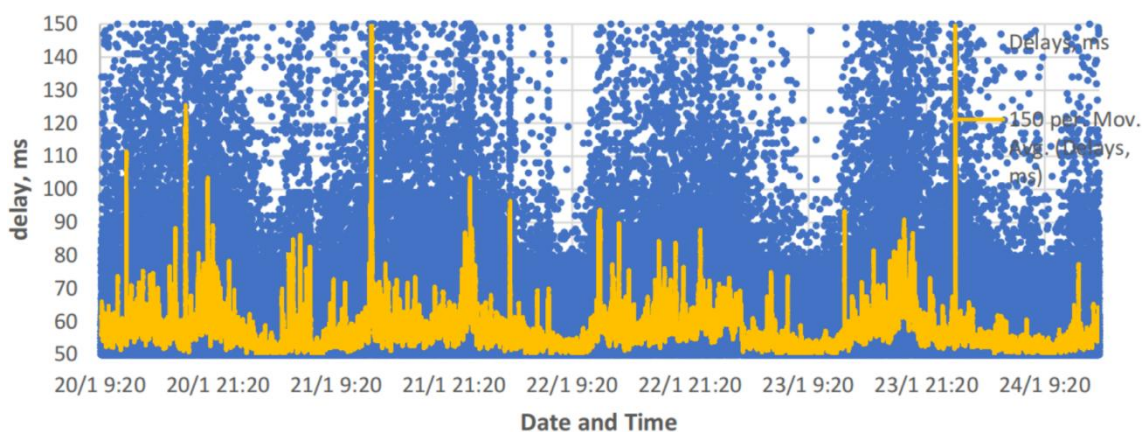


Figure 21. Delay values and Average delay in the LTE cell with a highly variable load.

As can be seen in Figure 21, there are fluctuations in the average delay, where its greatest values are observed during daytime, and smallest are at nights. As in the previous case, we will obtain estimates of the distribution parameters for the entire population of experimentally obtained delay values and assume that they are equal to the distribution parameters:  $\hat{\mu} = \mu = 4.006696531$ ,  $\hat{\sigma} = \sigma = 0.268607287$ . Now let's obtain the values of the distribution parameters point estimates using  $n = 50$  adjacent delay values. The point estimate values of the parameters  $\hat{\mu}_{50}$  and  $\hat{\sigma}_{50}$  will be illustrated on a two-dimensional graph in Figure 22. Further, for clarity, we will also show a confidence ellipse for parameter estimates with a confidence probability  $\beta = 0.997$ .

As can be seen, many of the parameter estimate values go beyond the confidence ellipse, and therefore the fluctuations in the values of the estimates, both  $\hat{\mu}_{50}$  and  $\hat{\sigma}_{50}$ , are not random.

Based on Figure 22, it may seem that the delay population in such a cell have a complex structure. However, by enlarging some time interval (see Figure 23), it becomes clear that in fact this is not entirely true.

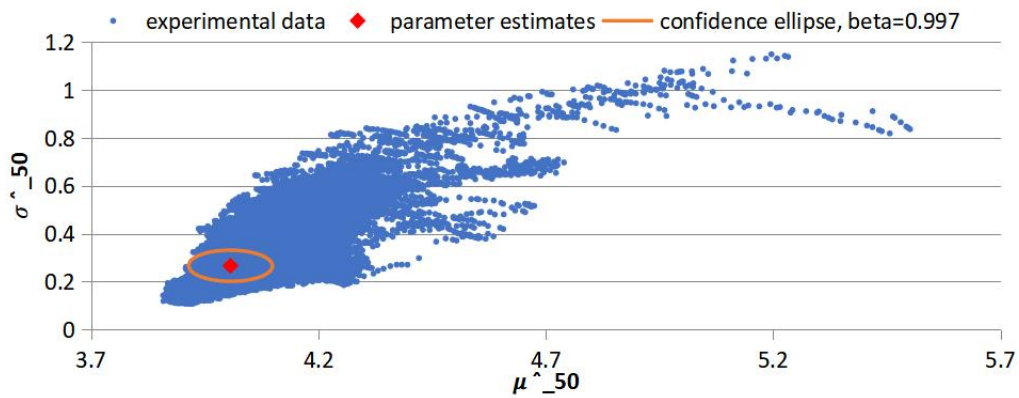


Figure 22. Parameter estimates from the experimental and simulated data in the LTE cell with a highly variable load.

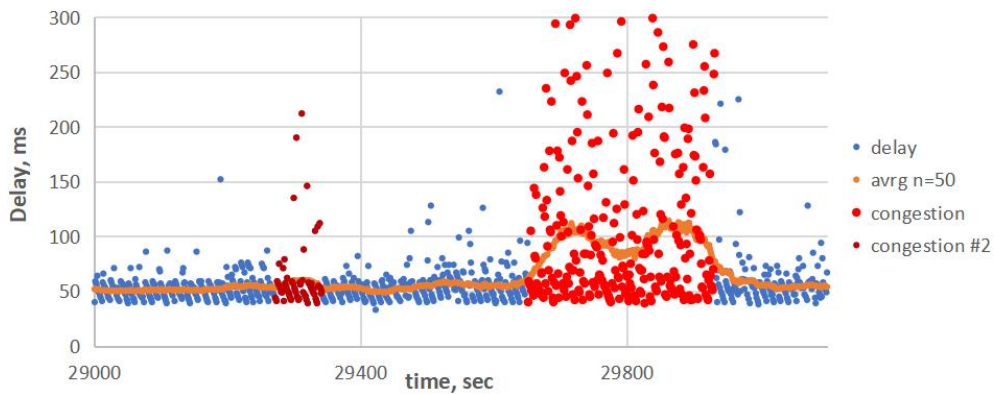


Figure 23. Delay values and Average delay in the LTE cell with a highly variable load (enlarged).

As can be seen from Figure 23, even in a cell operating with overloads, upon closer examination, it becomes obvious that there are time intervals when the delays are not increased, and their structure is not distorted; there are also periods of time when there is a sharp local increase in delays (see "jamming" in Figure 23), where there is not only a sharp increase in the average delay, but also a noticeable change in the structure of delay values. For each  $n = 50$  neighbor delay values, let's obtain estimates of the parameters  $\hat{\mu}_{50}$  and  $\hat{\sigma}_{50}$ , after which let's display them on a two-dimensional graph in Figure 24. Further, for clarity, let's impose a confidence ellipse, assuming that  $n = 50$  and the distribution parameters are equal to their estimates  $\hat{\mu} = \mu$  and  $\hat{\sigma} = \sigma$ , estimated at the time of the absence of congestion.

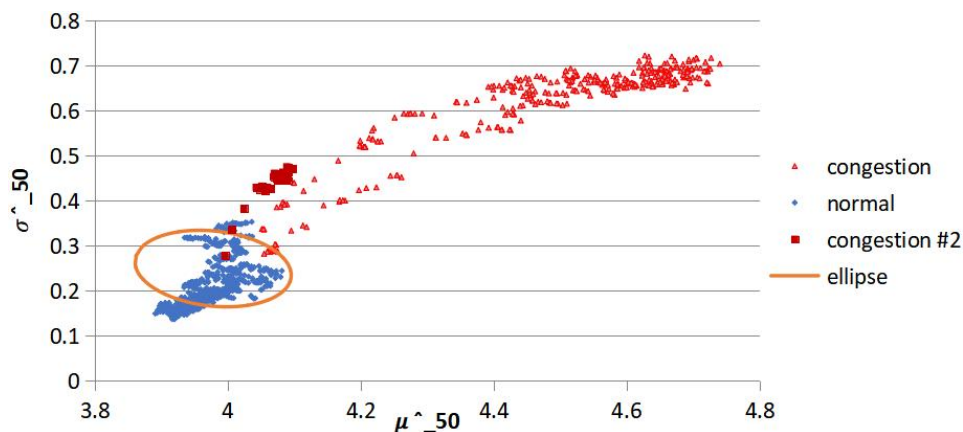


Figure 24. Parameters estimates during normal operation and congestion for  $n = 50$ .

Recall that, as illustrated in Figure 20, when a congestion occurs, the standard deviation estimates rise sharply in the first place. Then, with a closer analysis, using Figure 25, it becomes obvious that there are not one, but two congestions in the considered time interval. The parameter estimates obtained at the time of the smaller

(in magnitude and duration) congestion are designated as Congestion #2. For clarity, we also highlight these values in Figure 24 using same colours as in Figure 23.

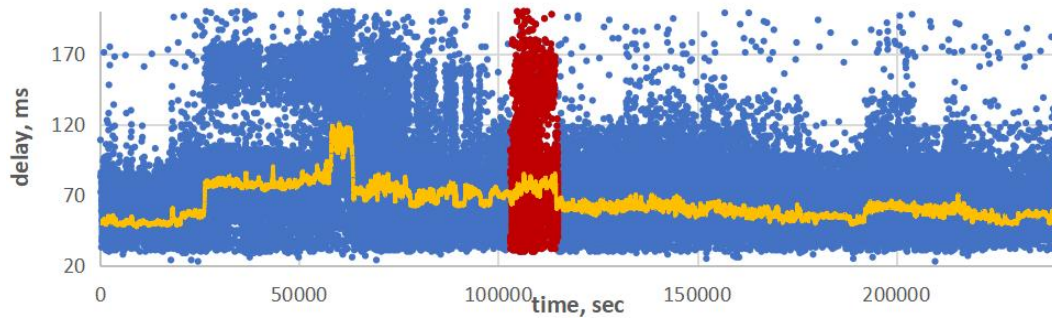


Figure 25. Delay values and Average delay in the LTE cell with various types of traffic.

Looking at Figure 23, it becomes clear that it is more difficult to visually determine small congestion in terms of duration and magnitude than using the estimates of the standard deviation illustrated in Figure 24.

### 3.5 Estimates of Delay Parameters in a Cell with Variations in Traffic Prioritization

Modern cellular mobile networks provide different levels of prioritization for different types of data traffic. Thus, low priority traffic may experience periods of increased both average delay and delays of retransmitted packets. At the same time, this phenomenon also manifests itself when the SINR is “good”. Figure 25 shows an example of delays in a cell operating within a university campus, and therefore the BS is forced to operate with highly variable traffic types, which, moreover, can often change both its composition and intensity. The delay measurements were made once per second throughout Friday, Saturday and Sunday. Delays were measured using 124 Bytes ICMP packets between UEs located at a distance of one meter from each other and registered in the same cell. The downlink SINR values were within the limits recommended in Table 1.

As can be seen, there are sharp changes in the composition of the delays. Let's take a closer look on Figure 26 at the area highlighted in red in Figure 25.

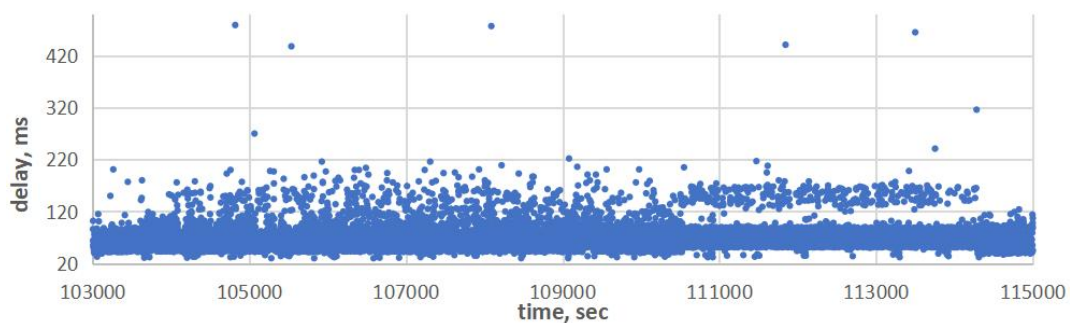


Figure 26. Delay values and Average delay in the LTE cell with various types of traffic (enlarged part).

As can be seen from Figure 27, the operation of a cell with different types of traffic and various load causes changes in both the structure of the delays and the estimates values of the delay parameters at these moments. At the same time, the transitions between different traffic compositions are not accompanied by increased values of delay parameter estimates  $\hat{\mu}_{50}$  and  $\hat{\sigma}_{50}$ .

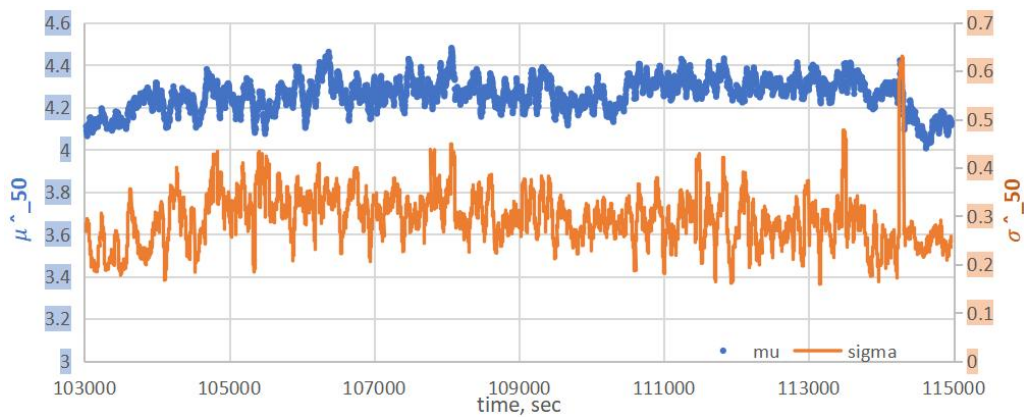


Figure 27. Running parameter estimates, obtained for  $n=50$  neighbour delay values.

## 4. Results and Discussions

Data transmission delays in a mobile cellular network in general are determined by the performance of the terrestrial backhaul network (which parameters are usually constant, but depend on the link implementation), as well as variable influencing factors such as signal quality (i.e. SINR), cell load, type of data traffic (traffic prioritization), etc. For this reason, UE-to-UE connection delays must be estimated for each cell separately, for which purpose both UEs must operate in the same cell when measuring delays. Processing of the data obtained from multiple cells can be done if the delays are processed for each cell separately.

When describing delays in a cell of a mobile cellular network using experimentally obtained data, one of the primary tasks is to obtain stable parameter estimates. To do this, it is necessary to neglect variable negative factors in order to consider estimates under stable operation of a cellular network. Further, if necessary, the impact of negative factors can be added additionally.

Air interface of modern cellular mobile networks operates with a relatively high block error rate (BLER). Terrestrial backhaul links of BSs may also occasionally experience congestion, so additional packet loss or packet reordering may occur. To reduce the number of lost packets, various retransmission techniques are implemented to protect different segments of the data path. The operation of such retransmission mechanisms affects the delay value and composition. To reduce the impact of retransmission mechanisms, we have chosen to use ICMP packets, which are protected only at the radio interface by the HARQ mechanism.

The air Interface data rate of a modern mobile cellular network depends on the selected modulation and coding scheme. The choice of modulation and coding is done automatically by the automatic modulation and coding (AMC) function based on the measured radio signal quality expressed in SINR values. Therefore, the delay values, among other things, depend on the SINR value too. In Chapter 2.1 we have demonstrated an approach to determining such dependence. In addition, we have shown an example using particular LTE UEs. It has been found that there are several ranges of SINR values where the effect of SINR on delay values can be considered constant and thus, if the SINR is in that range, it can be assumed that the signal quality does not affect the delay values. The most practical "good" SINR ranges are shown in *Table 1* for various packet sizes. Therefore, all experimental delay values obtained when the signal quality was not "good" must be discarded until parameter estimates are obtained.

In Chapter 2.2 we have shown how to anticipate, if necessary, the impact of "low" SINR values on average and maximum latency values. In addition, in Chapter 2.3, we have provided an example using particular LTE UEs, so the polynomial approximation coefficients from *Table 2* can be used to estimate the impact of "low" SINR on the delay values.

Public mobile cellular data services typically are operating with a mix of different types of data traffic. Since the load and composition of the traffic can vary greatly, and given the different levels of prioritization for different types of data traffic, the delays in a particular cell can have different values and structures. We have found several types of delay instabilities, which are listed and discussed in Chapter 3.

As shown in Chapter 3.3, delays can be significantly increased when the terrestrial backhaul line of a BS becomes **congested**. This can happen regardless of the downlink SINR value. The duration of such congestion can be up to several minutes, but the occurrence of such congestion is very rare. During such congestions, delays increase significantly. If the experimentally obtained delays are measured from a moving vehicle, then the duration of the measurement in a cell becomes comparable to the duration of a possible congestion.

Therefore, parameter estimates obtained from such experimental data will be significantly distorted and will not reflect the typical (at the time of the absence of a congestion) operation of a given cell. In order to be able to identify the occurrence of congestion during an experiment, the following properties can be used: (1) the estimate of the standard deviation will be significantly increased if it is estimated from the delays where the congestion starts or ends; (2) the skewness estimate would decrease (its value becomes close to zero or even negative) if it was estimated from the delays measured during congestion (in which case the standard deviation estimates would not increase so significantly). Because the probability of a congestion is low, the comparison of the "significant increase/decrease" of the estimates can be assessed by comparing the estimates obtained at different measurement times. Therefore, it is desirable to measure the delay in each cell at least twice at different times of the day.

Secondly, as discussed in Chapter 3.4, since the load in a public cell can be highly variable, the average delay in an overloaded cell do not just increase monotonically: **highly variable load** will cause multiple time periods with locally increased delays. In this case the parameter estimates become unstable. However, since the instability of the parameter estimates is caused by multiple overloads, the approach to identify congestions discussed above still can be applied. However, if there is no time when the cell is not suffering from congestion, using the current parameter estimates with  $n = \textit{several minutes}$  can be effective in determining where the congestion has occurred.

Thirdly, as demonstrated in Chapter 3.5, the varying composition of **traffic with different priorities** causes changes in the structure of delays. However, this does not lead to significant variations in the parameter estimate values of the expected value  $\hat{\mu}_{cell\_a}$  and standard deviation  $\hat{\sigma}_{cell\_a}$  estimates. Therefore, this phenomenon can be ignored when determining delay parameter estimates or can be identified by negative value of skewness  $\hat{Sk}_{cell\_a}$  parameter estimate.

## 5. Conclusion

The issues of obtaining stable estimated values of delay parameters in cells of a mobile cellular network with the aim of their further use for describing delays in a cell, assuming that there are no negative factors, is considered. An approach is shown to determine and an example using specific LTE equipment is shown the determination of the influence of radio signal quality on delay parameters and their stability. The "good" SINR ranges are given in the *Table 1*; the effect of the "low" SINR can be foreseen by using polynomial approximation using coefficient from *Table 2*.

Examples of congestion and its effect on delay parameters estimates of before, at the beginning, and during the congestion are given. The examples have been experimentally obtained using a real operating LTE cell. Signs are indicated by which, having expected, standard deviation and skewness estimates, can assume whether there was a congestion at the time of obtaining the delay values and thus whether these delay values should be excluded from the analysis to consider normal operation of a cell. Thus, if the estimates of the expected values  $\hat{\mu}_{cell\_a}$  obtained at different times in the same *cell\_a* are within the confidence interval per parameter, then the cell operates with an almost constant load, and therefore the delay values obtained at different times belong to the same general population and can be combined for further analysis. If it is required to exclude from the analysis the values of the estimates obtained at the time when the network was experiencing congestion, then all delay values whose standard deviation estimate  $\hat{\sigma}_{cell\_a}$  is sharply increased should be discarded. If it is required to exclude from the analysis the values of the estimates obtained at the time of a heavy load on the cell, then all delay values whose skewness estimate  $\hat{Sk}_{cell\_a}$  is close to zero or negative should be excluded.

## Conflict of Interest

There is no conflict of interest for this study.

## References

- [1] Karagiannis, G.; Altintas, O.; Ekici, E.; Heijenk, G.; Jarupan, B.; Lin, K.; Weil, T. Vehicular networking: A survey and tutorial on requirements, architectures, challenges, standards and solutions. *IEEE Commun. Sur*

- v. *Tutor*. **2011**, *4*, 584–616, <https://doi.org/10.1109/SURV.2011.061411.00019>.
- [2] Mir, Z.H.; Filali, F. LTE and IEEE 802.11p for vehicular networking: a performance evaluation. *EURASIP J. Wirel. Commun. Netw.* **2014**, *2014*, 89, <https://doi.org/10.1186/1687-1499-2014-89>.
- [3] Fotouhi, A.; Qiang, H.; Ding, M.; Hassan, M.; Giordano, L.G.; Garcia-Rodriguez, A.; Yuan, J. Survey on UAV Cellular Communications: Practical Aspects, Standardization Advancements, Regulation, and Security Challenges. *IEEE Commun. Surv. Tutor.* **2019**, *4*, 3417–3442, <https://doi.org/10.1109/COMST.2019.2906228>.
- [4] Mishra, D.; Natalizio, E. A survey on cellular-connected UAVs: Design challenges, enabling 5G/B5G innovations, and experimental advancements. *Comput. Netw.* **2020**, *182*, 107451, <https://doi.org/10.1016/j.comnet.2020.107451>.
- [5] ACJA, GSMA and GUTMA: LTE Aerial Profile v1.00. Available online: [https://www.gsma.com/iot/wp-content/uploads/2020/11/ACJA-WT3-LTE-Aerial-Profile\\_v1.00-2.pdf](https://www.gsma.com/iot/wp-content/uploads/2020/11/ACJA-WT3-LTE-Aerial-Profile_v1.00-2.pdf) / (accessed on 3 November 2020).
- [6] Zhu, H.; Rodríguez-Piñero, J.; Huang, Z.; Domínguez-Bolaño, T.; Cai, X.; Yin, X.; Lee, J. On the End-to-End Latency of Cellular-Connected UAV Communications. In Proceedings of 2021 15th European Conference on Antennas and Propagation (EuCAP), Dusseldorf, Germany, 22–26 March 2021, <https://doi.org/10.23919/EuCAP51087.2021.9411072>.
- [7] Zhou, H.; Hu, F.; Juras, M.; Mehta, A.B.; Deng, Y. Real-Time Video Streaming and Control of Cellular-Connected UAV System: Prototype and Performance Evaluation. *IEEE Wirel. Commun. Lett.* **2021**, *10*, 1657–1661, <https://doi.org/10.1109/lwc.2021.3076415>.
- [8] Gharib, M.; Nandadapu, S.; Afghah, F. An Exhaustive Study of Using Commercial LTE Network for UAV Communication in Rural Areas. In Proceedings of 2021 IEEE International Conference on Communications Workshops (ICC Workshops), Montreal, QC, Canada, 14–23 June 2021, <https://doi.org/10.1109/ICCWorkshops50388.2021.9473547>.
- [9] Luo, J.; Zhao, P.; Zheng, F.-C.; Li, L. Delay Evaluation for Cellular-Connected Drones: Experiments and Analysis. In Proceedings of 2022 IEEE 96th Vehicular Technology Conference (VTC2022-Fall), London, United Kingdom, 26–29 September 2022, <https://doi.org/10.1109/vtc2022-fall57202.2022.10012989>.
- [10] Brodnevs, D.; Kutins, A. Requirements of End-to-End Delays in Remote Control Channel for Remotely Piloted Aerial Systems. *IEEE Aerosp. Electron. Syst. Mag.* **2021**, *36*, 18–27, <https://doi.org/10.1109/maes.2020.3039853>.
- [11] 3GPP. 3GPP TS 22.125 Uncrewed Aerial System (UAS) support in 3GPP. Available online: <https://portal.3gpp.org/desktopmodules/Specifications/SpecificationDetails.aspx?specificationId=3545>. (accessed on 1 April 2022).
- [12] Tso, F.P.; Teng, J.; Jia, W.; Xuan, D. Mobility: A Double-Edged Sword for HSPA Networks: A Large-Scale Test on Hong Kong Mobile HSPA Networks. *IEEE Trans. Parallel Distrib. Syst.* **2011**, *23*, 1895–1907, <https://doi.org/10.1109/tpds.2011.289>.
- [13] Caushaj, E.; Ivanov, I.; Fu, H.; Sethi, I.; Zhu, Y. Evaluating Throughput and Delay in 3G and 4G Mobile Architectures. *J. Comput. Commun.* **2014**, *02*, 1–8, <https://doi.org/10.4236/jcc.2014.210001>.
- [14] Putra, G.M.; Budiman, E.; Malewa, Y.; Cahyadi, D.; Taruk, M.; Hairah, U. 4G LTE Experience: Reference Signal Received Power, Noise Ratio and Quality. In Proceedings of 2021 3rd East Indonesia Conference on Computer and Information Technology (EIConCIT), Surabaya, Indonesia, 9–11 April 2021, <https://doi.org/10.1109/EIConCIT50028.2021.9431853>.
- [15] Zulkifley, M.A.; Behjati, M.; Nordin, R.; Zakaria, M.S. Mobile Network Performance and Technical Feasibility of LTE-Powered Unmanned Aerial Vehicle. *Sensors* **2021**, *21*, 2848, <https://doi.org/10.3390/s21082848>.
- [16] Metsala, E.; Salmelin, J. *Mobile Backhaul*. John Wiley & Sons: Hoboken, NJ, USA, 2012; pp. 346–351.
- [17] Laner, M.; Svoboda, P.; Romirer-Maierhofer, P.; Nikaein, N.; Ricciato, F.; Rupp, M. A Comparison Between One-way Delays in Operating HSPA and LTE Networks. In Proceedings of 2012 10th International Symposium on Modeling and Optimization in Mobile, Ad Hoc and Wireless Networks (WiOpt), Paderborn, Germany, 14–18 May 2012.
- [18] Morales, J.; Rodríguez, G.; Akopian, D.; Huang, G. Toward UAV control via cellular networks: Delay Profiles, Delay Modeling, and a Case Study within the 5-mile Range. *IEEE Trans. Aerosp. Electron. Syst.* **2020**, *5*, 4132–4151, <https://doi.org/10.1109/TAES.2020.2987406>.
- [19] Uitto, M.; Heikkinen, A. Evaluation of live video streaming performance for low latency use cases in 5G. In Proceedings of 2021 Joint European Conference on Networks and Communications & 6G Summit (EuCN

- C/6G Summit), Porto, Portugal, 8–11 June 2021, <https://doi.org/10.1109/EuCNC/6GSummit51104.2021.9482605>.
- [20] Rischke, J.; Sossalla, P.; Itting, S.; Fitzek, F.H.P.; Reisslein, M. 5G Campus Networks: A First Measurement Study. *IEEE Access* **2021**, *9*, 121786–121803, <https://doi.org/10.1109/access.2021.3108423>.
- [21] Stuhlfauth, R. *High Speed Packet Access*, First Edit. Rohde&Schwarz: Singapore, Singapore, 2012; pp. 9–13, 145–149.
- [22] Imoize, A.L.; Tofade, S.O.; Ughegbe, G.U.; Anyasi, F.I.; Isabona, J. Updating analysis of key performance indicators of 4G LTE network with the prediction of missing values of critical network parameters based on experimental data from a dense urban environment. *Data Brief* **2022**, *42*, <https://doi.org/10.1016/j.dib.2022.108240>.
- [23] Kutins, A.; Brodnevs, D. Determination of Delay Parameters in 4G LTE Cellular Mobile Networks. In Proceedings of 2022 Workshop on Microwave Theory and Techniques in Wireless Communications (MTTW), Riga, Latvia, 5–7 October 2022, <https://doi.org/10.1109/MTTW56973.2022.9942617>.
- [24] 3GPP TR 36.777. Enhanced LTE support for aerial vehicles. Available online: <https://portal.3gpp.org/desktopmodules/Specifications/SpecificationDetails.aspx?specificationId=3231>. (accessed on 12 October 2018).
- [25] Trinh, H.D.; Zeydan, E.; Giupponi, L.; Dini, P. Detecting Mobile Traffic Anomalies Through Physical Control Channel Fingerprinting: A Deep Semi-Supervised Approach. *IEEE Access* **2019**, *7*, 152187–152201, <https://doi.org/10.1109/access.2019.2947742>.
- [26] Kim, C.; Mendiratta, V.B.; Thottan, M. Unsupervised Anomaly Detection and Root Cause Analysis in Mobile Networks. In Proceedings of 2020 International Conference on COMMunication Systems & NETWORKS (COMSNETS), Bengaluru, India, 7–11 January 2020, <https://doi.org/10.1109/COMSNETS48256.2020.9027328>.
- [27] Ahmed, A.H.; Hicks, S.; Riegler, M.A.; Elmokashfi, A. Predicting High Delays in Mobile Broadband Networks. *IEEE Access* **2021**, *9*, 168999–169013, <https://doi.org/10.1109/access.2021.3138695>.
- [28] Yamamoto, K.; Wakamiya, N.; Nakano, R.; Fujiwara, R. Model-based anomaly detection in response delay in communication through LTE network. In Proceedings of 2021 22nd Asia-Pacific Network Operations and Management Symposium (APNOMS), Tainan, Taiwan, 8–10 September 2021, <https://doi.org/10.23919/APNOMS52696.2021.9562666>.